Inorg. Chem. **2006**, *45*, 1439–1441

Inorganic Chemistry
Communication

Layer-by-Layer Deposition of Bimetallic Nanoshells on Functionalized Polystyrene Beads

Snigdhamayee Praharaj, Sudip Nath, Sudipa Panigrahi, Sujit Kumar Ghosh, Soumen Basu, Surojit Pande, Subhra Jana, and Tarasankar Pal*

Department of Chemistry, Indian Institute of Technology, Kharagpur 721302, India

Received November 6, 2005

Bimetallic nanoshells on functionalized polystyrene beads have been fabricated through a layer-by-layer deposition technique exploiting electrostatic interaction. The synthesis has been achieved through the immobilization and successive reduction of the corresponding precursor ions. It has been shown that the thickness of the shell can be controlled by a number of cyclic depositions of respective metals onto the surface of the polystyrene beads.

Inorganic-nanoshell-coated organic polystyrene beads with well-defined architectures are of increasing interest because of their applications in the fields of surface-enhanced Raman scattering (SERS),[1] catalysis,[2] biochemistry,[3] etc. These hybrid materials are found to be useful in the area of advanced microelectronic devices, nonlinear optics, electrochemical sensors, bioanalysis, chemical sensors, and capsules for the controlled release of therapeutic agents.[4] These supported nanomaterials are of special interest because they allow fine dispersion and stabilization of small metallic particles[5,6] and provide access to a larger number of catalytically active sites[7] than the corresponding bulk components. The core–shell-type composite materials are in the frontier of advanced research, in which the shell component determines the surface properties of the particles and the core material indirectly induces other (optical, catalytic, magnetic, etc.)[8,9] properties of the system. Moreover, tailoring of bimetallic catalysts is an important factor because of their good selectivity toward the desired reaction as a consequence of the electronic and ensemble effects of two metals.[10] The fabrication of polystyrene$_{\text{core}}$–metal$_{\text{shell}}$ composites is of special interest, and a few ingenious methods have been reported to design them.[11,12] However, most of the cases result in either a thick metal coating with irregular thickness or a large number of uncoated particles due to Coulombic repulsion and surface passivation.[11]

Scheme 1. Schematic Representation of the Synthesis of $[R(Au^0)(Pd^0)]^+Cl^-$

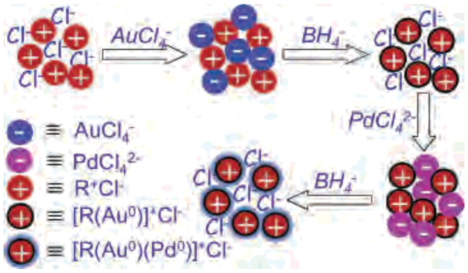

Herein we report a layer-by-layer deposition technique to fabricate ultrathin bimetallic nanoshells on functionalized polystyrene beads exploiting electrostatic interaction and suggest their consideration. An ion-exchange mechanism was primarily involved to immobilize the metal precursors, which upon subsequent reduction form a bimetallic coating on the functionalized polystyrene beads. The particles were characterized by scanning electron microscopy (SEM), energy-dispersive X-ray (EDX) analysis, X-ray photoelectron spectroscopy (XPS), and X-ray diffraction (XRD) studies. To the best of our knowledge, this is the first report to synthesize bimetallic-nanoshell-coated polystyrene beads in a layer-by-layer fashion.

The bimetallic coating on functionalized anion-exchange resin beads was fabricated by involving a synthetic strategy as shown in Scheme 1. For the synthesis of gold–palladium-coated resin beads, 1 g of the anion-exchange resin, SERALITE-SRA-400 (in chloride form), was treated with 5 mL of 10^{-2} M $HAuCl_4$ and stirred on a magnetic stirrer for

---

* To whom correspondence should be addressed. E-mail: tpal@chem.iitkgp.ernet.in.

(1) Cheng, W.; Dong, S.; Wang, E. *J. Phys. Chem. B* **2004**, *108*, 19146.
(2) Chen, C. W.; Serizawa, T.; Akashi, M. *Chem. Mater.* **1999**, *11*, 1381.
(3) Siiman, O.; Burshteyn, A. *J. Phys. Chem. B* **2000**, *104*, 9795.
(4) Lu, C.; Wu, N.; Jiao, X.; Luo, C.; Cao, W. *Chem. Commun.* **2003**, 1056.
(5) Pol, V. G.; Grisaru, H.; Gedanken, A. *Langmuir* **2005**, *21*, 3635.
(6) Worden, J. G.; Shaffer, A. W.; Huo, Q. *Chem. Commun.* **2004**, 518.
(7) Praharaj, S.; Nath, S.; Ghosh, S. K.; Kundu, S.; Pal, T. *Langmuir* **2004**, *20*, 9889.
(8) Liz-Marzan, L. M.; Kamat, P. V. *Nanoscale Materials*; Kluwer Academic Publishers: Norwell, MA, 2003.
(9) Nath, S.; Ghosh, S. K.; Kundu, S.; Praharaj, S.; Panigrahi, S.; Basu, S.; Pal, T. *Mater. Lett.* **2005**, *59*, 3986.
(10) Ruban, A. V.; Skriver, H. L.; Nørskov, J. K. *Phys. Rev. B* **1999**, *59*, 15990.
(11) Wescott, S. L.; Oldenburg, S. J.; Lee, T. R.; Halas, N. J. *Langmuir* **2000**, *16*, 6921.
(12) Caruso, F.; Caruso, R. A.; Mohwald, H. *Science* **2001**, *105*, 2743.

10.1021/ic051915n CCC: $33.50

complete exchange of Cl^- ions with $AuCl_4^-$ ions. Within 2 h, the solution above the beads became colorless. Afterward, the resin-bound $AuCl_4^-$ moiety, i.e., $[R-AuCl_4]$, was washed with distilled water, dried, and finally reduced by a freshly prepared $NaBH_4$ solution. The product was a gold-nanoshell-coated resin bead, $[R(Au^0)]^+Cl^-$. A total of 5 mL of a 10^{-2} M aqueous solution of H_2PdCl_4 was added to the preformed $[R(Au^0)]^+Cl^-$, and the mixture was stirred again on the magnetic stirrer. The solution above the bead became colorless within 2−3 h, indicating the ready exchange of $PdCl_4^{2-}$ with the Cl^- of $[R(Au^0)]^+Cl^-$. The addition of freshly prepared $NaBH_4$ results in a black gold−palladium-coated bead, $[R(Au^0)(Pd^0)]^+Cl^-$.

Anionic precursor $AuCl_4^-$ was exchanged with the Cl^- ion of the resin (R^+Cl^-) through an ion-exchange mechanism and initiated the synthesis. The anion-exchange resin has a positive functional group, $-N(CH_3)_3^+$, which can bind $AuCl_4^-$ electrostatically to form $[R-AuCl_4]$. Now upon subsequent reduction, the resin-bound gold chloride moiety was converted to gold-coated resin beads, $[R(Au^0)]^+Cl^-$. To maintain the electroneutrality of the matrix, the Cl^- remained bonded to the positive entity $[R(Au^0)]^+$, which was authenticated from EDX analysis. Now the addition of a $PdCl_4^{2-}$ solution to $[R(Au^0)]^+Cl^-$ followed by reduction leads to the formation of a palladium nanoshell on the gold-coated resin beads, represented as $[R(Au^0)(Pd^0)]^+Cl^-$. The following reactions are involved during the synthesis of the particles.

$$R^+Cl^- + HAuCl_4 \rightarrow [R-AuCl_4] + HCl$$

$$[R-AuCl_4] \xrightarrow{[H]} [R(Au^0)]^+Cl^-$$

$$[R(Au^0)]^+Cl^- + H_2PdCl_4 \rightarrow [R(Au^0)]_2{}^{2+}PdCl_4{}^{2-} + HCl$$

$$[R(Au^0)]_2{}^{2+}PdCl_4{}^{2-} \xrightarrow{[H]} [R(Au^0)(Pd^0)]^+Cl^-$$

The exchange of $PdCl_4^{2-}$ was authenticated by adding dilute HCl to the $[R(Au^0)]_2^{2+}PdCl_4^{2-}$ beads. The colorless HCl solution above the resin bead turned yellow, showing the characteristic absorption band of H_2PdCl_4 at 398 nm.

The layer-by-layer deposition of metals on a functionalized cation-exchange resin was done by employing the same synthetic protocol. Cationic complexes $[Ag(NH_3)_2]^+$ and $[Cu(NH_3)_4]^{2+}$ were used as silver and copper precursors, respectively, for the fabrication of $[R(Ag^0)(Cu^0)]^-H^+$ particles (see the Supporting Information). The sulfonate functionality ($-SO_3^-$) of the cation-exchange resin leads to electrostatic attachment of the cationic precursors.

In the case of core−shell bimetallic nanoparticle synthesis, the more noble metal usually forms the core and the less one forms the shell. In contrast, the construction of an inverted structure is not easy because the less noble metal is solubilized by a redox reaction upon the addition of more noble metal ions.[13] The above synthetic strategy leads to easy generation of $[R(Ag^0)(Cu^0)]^-H^+$ and $[R(Au^0)(Pd^0)]^+Cl^-$ nanocomposites with their inverted structures. The order of deposition of the bimetallic shells on the polystyrene beads can be altered by the successive immobilization of their corresponding precursors. The matrixes such as $[R(Pd^0)(Pt^0)]^+Cl^-$ and $[R(Ag^0)(Au^0)]^+Cl^-$ were also synthesized from their corresponding metal chloride precursors.

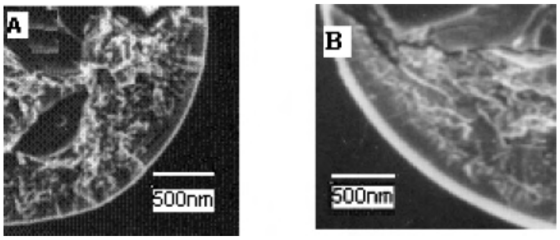

Figure 1. HRSEM micrographs of a single (A) $[R(Au^0)]^+Cl^-$ and (B) $[R(Au^0)(Pd^0)]^+Cl^-$.

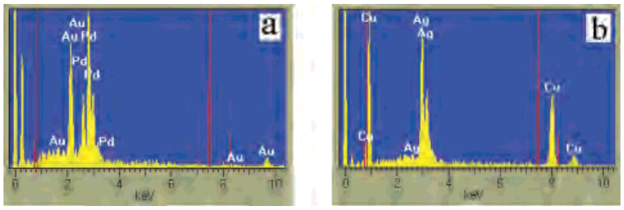

Figure 2. EDX spectra of (a) $[R(Au^0)(Pd^0)]^+Cl^-$ and (b) $[R(Ag^0)(Cu^0)]^-H^+$.

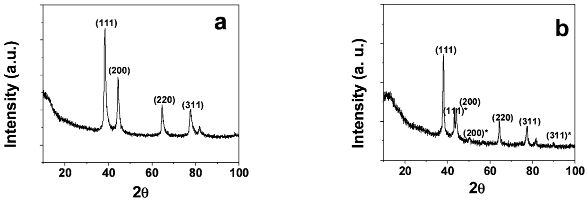

Figure 3. XRD patterns of (a) $[R(Au^0)(Pd^0)]^+Cl^-$ and (b) $[R(Ag^0)(Cu^0)]^-H^+$.

The layer-by-layer deposition technique has been widely used to fabricate core−shell particles because of its convenience to tailor the thickness and composition of the shells. The thickness can be controlled by varying the number of cycles of operation: immobilization and subsequent reduction. In this way, we can deposit more than two metals on any kind of charged polystyrene bead.

The high-resolution SEM (HRSEM) images of cross-sectional views of $[R(Au^0)]^+Cl^-$ and $[R(Au^0)(Pd^0)]^+Cl^-$ particles are shown in parts A and B of Figure 1, respectively. The figures clearly depict the thickness of monometallic gold (50 ± 5 nm) and bimetallic gold−palladium (90 ± 5 nm) shells. The images show a stepwise increase in the size of the resin bead with layer-by-layer deposition of metals. The EDX patterns of the composite materials $[R(Au^0)(Pd^0)]^+Cl^-$ and $[R(Ag^0)(Cu^0)]^-H^+$ are shown in Figure 2. The EDX patterns of monometallic-coated resin beads are given in the Supporting Information.

The XRD patterns of $[R(Ag^0)(Cu^0)]^-H^+$ and $[R(Au^0)(Pd^0)]^+Cl^-$ show information about the nature of the metals coated on polystyrene beads. The XRD of $[R(Au^0)(Pd^0)]^+Cl^-$ (Figure 3 a) shows the peaks at 38.2, 44.4, 64.65, and 77.9° assigned to the (111), (200), (220), and (311) reflection planes, respectively, which substantiates the face-centered-cubic nature of Au nanocrystals. The absence of sharp

---

(13) Toshima, N.; Shiraishi, Y.; Shiotsuki, A.; Ikenaga, D.; Wang, Y. *Eur. Phys. J. D* **2001**, *16*, 209.

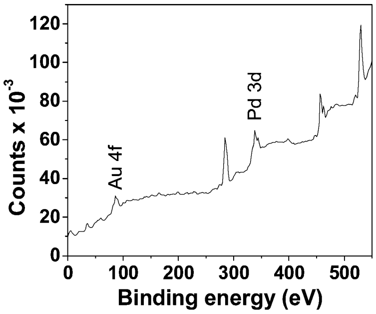

Figure 4. XPS image of $[R(Au^0)(Pd^0)]^+Cl^-$ particles.

scattering peaks for Pd may be due to the weak diffraction of Pd.[14] The XRD of $[R(Ag^0)(Cu^0)]^-H^+$ particles shows diffraction peaks at 38.05, 44.1, 64.4, and 77.45° assigned to (111), (200), (220), and (311) planes of Ag, respectively, and the peaks at 43.2, 50.37, and 89.9 correspond to the (111), (200), and (311) planes of Cu, respectively, as shown in Figure 3b.

The oxidation states of the metals coated on resin beads were investigated by XPS. The XPS of $[R(Au^0)(Pd^0)]^+Cl^-$ (Figure 4) shows a spectral profile completely different from that of R^+Cl^- (see the Supporting Information). The intense peaks at 83 and 86.5 eV correspond to the binding energies of Au $4f_{7/2}$ and $4f_{5/2}$ electrons, respectively, and those at 338.5 and 343 eV depict those of Pd $3d_{5/2}$ and $3d_{3/2}$ electrons, respectively.[15] The shifting of the peaks as compared to the literature value may be due to the deposition of the metals on the surface of charged polystyrene beads. These data delineate the zero oxidation states of the metals.

The electrostatic field of attraction on the surface of the composites with variable metallic thickness was examined by the ready adsorption of a colored water-soluble complex ion, $[Cu(NH_3)_4]^{2+}$, on the composite surfaces. After a certain time interval, a decrease in the absorbance value of the solution was observed, depending on the thickness of the metallic layers. In this context, metal-coated resins $[R(Ag^0)]^-H^+$ and $[R(Ag^0)(Cu^0)]^-H^+$ and an equal amount of the uncoated $[R^-H^+]$ materials were separately mixed with the same amount of a $[Cu(NH_3)_4]SO_4$ solution. The absorbance values of the supernatant for all of the three mixtures were measured after a certain time (1 h) using the UV−visible spectrophotometer (Figure 5).

The change in the absorbance value was noticed as a consequence of the different extent of adsorption of the complex depending on the types of particles. This effect is a mere reflection of the extent of electrostatic attraction between charged polystyrene beads and the complex solution.

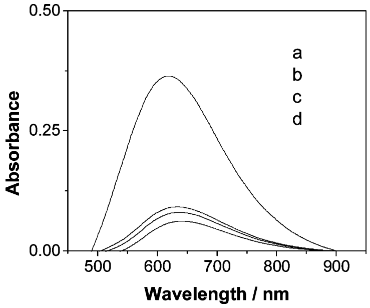

Figure 5. UV−visible spectra of an aqueous $[Cu(NH_3)_4]^{2+}$ solution after treatment with (a) no particles, (b) $[R(Ag^0)(Cu^0)]^-H^+$, (c) $[R(Ag^0)]^-H^+$, and (d) R^-H^+.

It was noted that, as the thickness of the shell increases, the extent of adsorption of $[Cu(NH_3)_4]^{2+}$ decreases. So, the absorbance value of the supernatant was highest for the solution containing the $[R(Ag^0)(Cu^0)]^-H^+$ matrix and lowest for the $[R^-H^+]$ case. This ionic interaction depends on the ionic charge and the distance of closest approach between the charged polystyrene beads and the $[Cu(NH_3)_4]^{2+}$ ionic species.[16]

In conclusion, a layer-by-layer deposition technique has been developed to fabricate bimetallic-nanoshell-coated functionalized polystyrene beads. The electrostatic field force has been exploited for the immobilization of the precursor ions to the resin moiety. The procedure is simple and reproducible and could be a general strategy for the synthesis of multimetallic nanoshells on any kind of charged polystyrene beads. The deposition of metals on the spherical polystyrene support can be done by the proper choice of the functional group of the resin beads and charge of the precursor. The synthesis of such particles along with their inverted structure can be achieved easily irrespective of the nobility of the metals. The synthesized composite materials are expected to be beneficial for SERS studies. These particles have already shown promise as heterogeneous catalysts in several redox reactions.[7] Finally, such bimetallic coatings on functionalized polystyrene beads are expected to open some new avenues in the application of optical studies, catalysis, and biochemical separation for their tunable features in relation to their shell thickness, material composition, and electrostatic field force from within.

Acknowledgment. The authors are thankful to UGC, DST, and CSIR, New Delhi, India, and IIT, Kharagpur, India, for financial assistance.

Supporting Information Available: EDX, XRD, and XPS analyses and brief explanations. This material is available free of charge via the Internet at http://pubs.acs.org.

IC051915N

---

(14) Mizukoshi, Y.; Okitsu, K.; Maeda, Y.; Yamamoto, T. A.; Oshima, R.; Nagata, Y. *J. Phys. Chem. B* **1997**, *101*, 7033.

(15) Chrastain, J., King, R. C., Eds. *Handbook of X-ray Photoelectron Spetroscopy*; Physical Electronics, Inc.: Minneapolis, MN, 1995.

(16) Peppas, N. A.; Khare, A. R. *Adv. Drug Delivery Rev.* **1993**, *11*, 1.